Simulation of the elastic properties of some fibre-reinforced composite laminates under off-axis loading system

S. VLASE, H. TEODORESCU-DRAGHICESCU[*], M. R. CALIN[a], L. SERBINA[a]
Transilvania University of Brasov, Department of Mechanics, 29 Eroilor Blvd, 500036 Brasov, Romania
[a]"Horia Hulubei" National Institute of Physics and Nuclear Engineering - IFIN HH, P.O. Box MG-6, 077125, Magurele, Romania

The paper presents simulations regarding the elastic properties of glass, carbon and Kevlar49 fibre-reinforced composite laminates based on epoxy resin and subjected to off-axis loading system using an approach developed by Clyne and Withers within Cambridge University, UK [13]. Following composite laminates with HM-carbon, HS-carbon and Kevlar49 fibres with plies sequence [0/90/0/90], [0/45/-45/90] and [45/-45/45/-45] as well as E-glass fibres-reinforced laminates with plies sequence [16/-81.8], [30/-30/90], [55/-55] have been used in simulations. The glass fibres laminates with the above plies sequence are commonly used to withstand the inner pressure of composite tubes and tanks. The elastic constants as well as the tensile-shear interaction have been determined. In order to obtain equal stiffness in all off-axis loading systems, a composite laminate has to present balanced angle plies. A comparison between the elastic properties of these laminates and the quasiisotropic ones is presented. Tensile-shear interaction in a fibre-reinforced composite laminate occurs only if the off-axis loading system does not coincide with the main axes of a single lamina or if the laminate is not balanced.

(Received March 18, 2011; accepted April 11, 2011)

Keywords: Carbon fibres, Glass fibres, Off-axis loadings, Composite laminates, Elastic properties

1. Introduction

It is well known that composite laminates with aligned reinforcement are very strong along the fibres but also very weak transverse to the fibres direction. This fact is more obvious in the case of advanced composite laminates reinforced with anisotropic carbon or aramid fibres such as HM-carbon, HS-carbon and Kevlar49 but this is fair accurate for glass fibre-reinforced laminates too [1-3]. Getting equal stiffness of laminates is a demand, so in general, the solution to obtain equal stiffness of laminates subjected in all directions within a plane is to stack and bond together plies with different fibres orientations [4-6]. Simulating elastic properties of fibre-reinforced composite laminates is for a great importance in designing composite structures especially suited for aerospace, defence and automotive industries, but also for transportation, chemistry and food industries [7-10]. Carbon fibres of type HM (high modulus) present a value of Young's modulus greater than 300 GPa. High strength (HS) carbon fibres are for general purposes, cost effective designed for industrial and recreational applications and are usually used for non-structural components of aircrafts. Kevlar 49 aramid fibre is characterized by low-density and high-tensile strength and modulus. These properties are the key to its successful use as reinforcement for plastic composite structures in aircraft, aerospace, marine, automotive, other industrial applications, and in sports equipment. It is available in continuous-filament yarns, chopped fibres, woven and unidirectional fabrics, tissues or veils and tapes for reinforcement applications. Kevlar 49 aramid is used in high-performance composite applications where lightweight, high strength and stiffness, vibration damping and resistance to damage and fatigue are for a great importance. Reinforced composite structures can save up to 40% of the weight of glass-fibre composites at equivalent stiffness [11-12].

2. A theoretical approach

A composite laminate (Fig. 1) formed by a number of unidirectional reinforced laminae subjected regarding to the loading scheme presented in Fig. 2 is considered. The elasticity law for a unidirectional lamina K can be expressed as following:

$$\begin{bmatrix} \sigma_{xx\,K} \\ \sigma_{yy\,K} \\ \tau_{xy\,K} \end{bmatrix} = \begin{bmatrix} r_{11K} & r_{12K} & r_{13K} \\ r_{12K} & r_{22K} & r_{23K} \\ r_{13K} & r_{23K} & r_{33K} \end{bmatrix} \cdot \begin{bmatrix} \varepsilon_{xx\,K} \\ \varepsilon_{yy\,K} \\ \gamma_{xy\,K} \end{bmatrix}, \qquad (1)$$

where r_{ijK} represent the transformed stiffness, σ_{xxK} , σ_{yyK} are the mean stresses of K lamina on x- respective y-axis and τ_{xyK} represent the mean shear stress of K lamina against the x-y coordinate system. The balance equations for the composite laminate are:

$$n_{xx} = \underline{\sigma}_{xx} \cdot t = \sum_{K=1}^{N} \left(\sigma_{xxK} \cdot t_K \right) = \sum_{K=1}^{N} n_{xxK} \ , \qquad (2)$$

$$n_{yy} = \underline{\sigma}_{yy} \cdot t = \sum_{K=1}^{N} \left(\sigma_{yyK} \cdot t_K \right) = \sum_{K=1}^{N} n_{yyK} \,, \qquad (3)$$

$$n_{xy} = \underline{\tau}_{xy} \cdot t = \sum_{K=1}^{N} \left(\tau_{xyK} \cdot t_K \right) = \sum_{K=1}^{N} n_{xyK} \,, \qquad (4)$$

where n_{xx} , n_{yy} are the normal forces on the unit length of the laminate on x- respective y-axis and n_{xy} represents the shear force, in plane, on the unit length of the laminate against the x-y coordinate system. $\underline{\sigma}_{xx}$, $\underline{\sigma}_{yy}$ are the normal stresses on x- respective y-axis of the laminate, $\underline{\tau}_{xy}$ represent the shear stress of the laminate against the x-y coordinate system. t_K , t represent the thickness of the K lamina respective the laminate thickness, n_{xxK} , n_{yyK} are forces on the unit length of K lamina on x- respective y-axis directions and n_{xyK} is the shear force in plane, on the unit length of K lamina against the x-y coordinate system. Beside the balance equations, the geometric conditions to compute the stresses must be determined too.

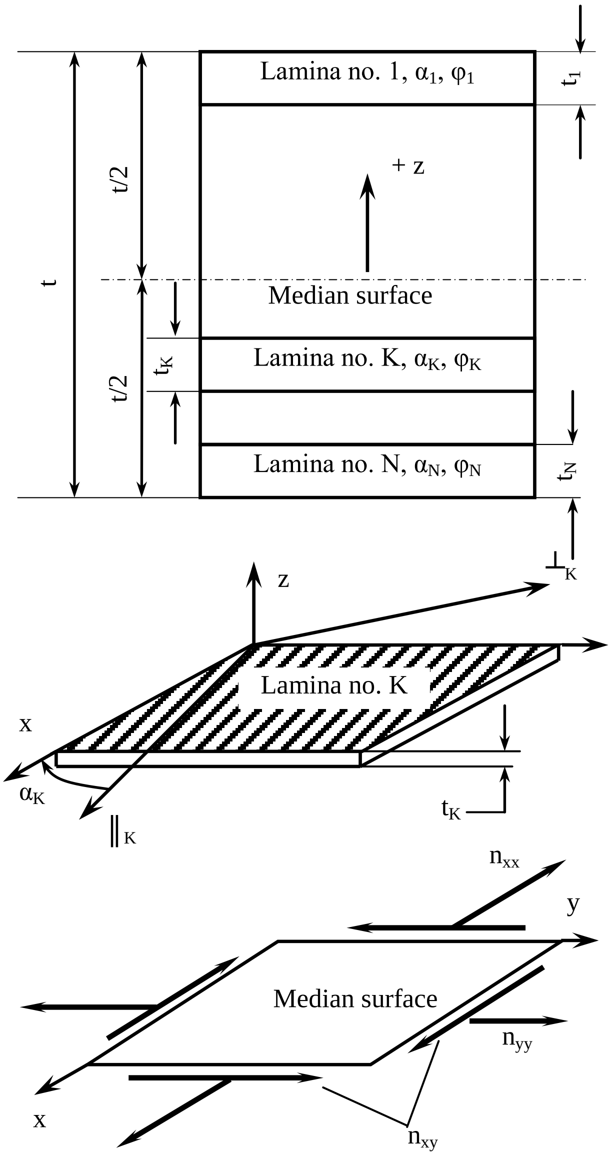

Fig. 1. Constructive scheme of a composite laminate.

For composite laminates, these geometric conditions imply that all laminae are bonded together and withstand, in a specific point, the same strains ε_{xx}, ε_{yy}, γ_{xy} as well as for the entire laminate.

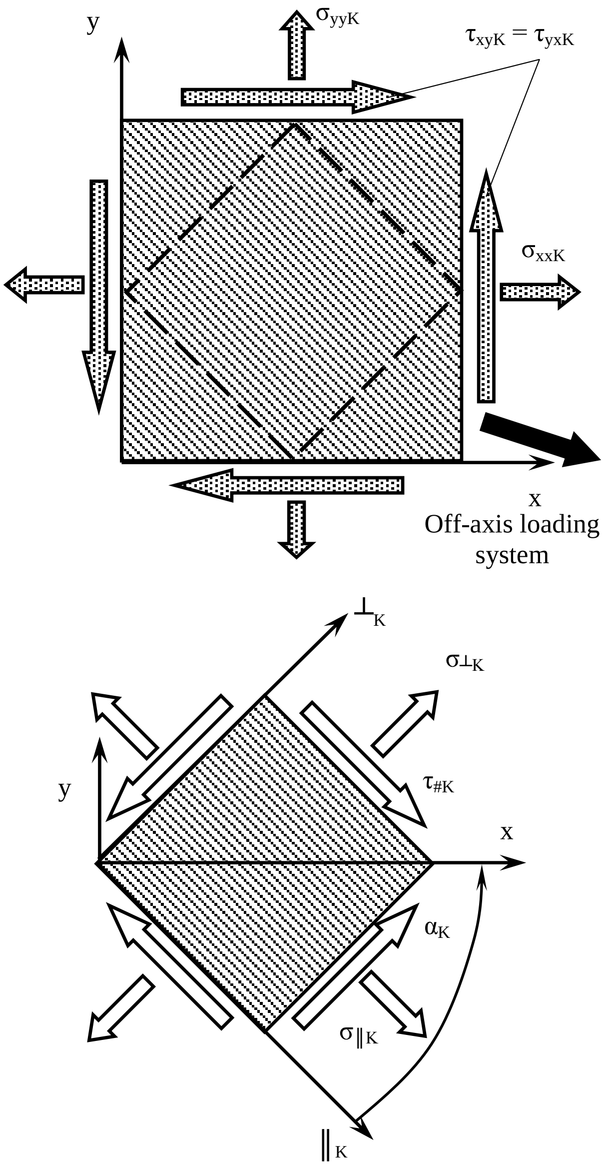

Fig. 2. Loading scheme of a composite laminate.

The geometric conditions are:

$$\begin{aligned} \varepsilon_{xxK} &= \varepsilon_{xx} \,, \\ \varepsilon_{yyK} &= \varepsilon_{yy} \,, \\ \gamma_{xyK} &= \gamma_{xy} \,, \end{aligned} \qquad (5)$$

for all K laminae.

According to equations (1)-(5), the elasticity law for entire laminate can be computed:

$$\begin{bmatrix} \underline{\sigma}_{xx} \\ \underline{\sigma}_{yy} \\ \underline{\tau}_{xy} \end{bmatrix} = \begin{bmatrix} \sum_{K=1}^{N}\left(r_{11K}\cdot\frac{t_K}{t}\right) & \sum_{K=1}^{N}\left(r_{12K}\cdot\frac{t_K}{t}\right) & \sum_{K=1}^{N}\left(r_{13K}\cdot\frac{t_K}{t}\right) \\ \sum_{K=1}^{N}\left(r_{12K}\cdot\frac{t_K}{t}\right) & \sum_{K=1}^{N}\left(r_{22K}\cdot\frac{t_K}{t}\right) & \sum_{K=1}^{N}\left(r_{23K}\cdot\frac{t_K}{t}\right) \\ \sum_{K=1}^{N}\left(r_{13K}\cdot\frac{t_K}{t}\right) & \sum_{K=1}^{N}\left(r_{23K}\cdot\frac{t_K}{t}\right) & \sum_{K=1}^{N}\left(r_{33K}\cdot\frac{t_K}{t}\right) \end{bmatrix} \cdot \begin{bmatrix} \varepsilon_{xx} \\ \varepsilon_{yy} \\ \gamma_{xy} \end{bmatrix}, \quad (6)$$

where the laminate stiffness $\underline{r}_{ij}$ are:

$$\underline{r}_{ij} = \sum_{K=1}^{N}\left(r_{ijK}\cdot\frac{t_K}{t}\right). \quad (7)$$

So, the laminate elasticity law becomes:

$$\begin{bmatrix} \underline{\sigma}_{xx} \\ \underline{\sigma}_{yy} \\ \underline{\tau}_{xy} \end{bmatrix} = \begin{bmatrix} \underline{r}_{11} & \underline{r}_{12} & \underline{r}_{13} \\ \underline{r}_{12} & \underline{r}_{22} & \underline{r}_{23} \\ \underline{r}_{13} & \underline{r}_{23} & \underline{r}_{33} \end{bmatrix} \cdot \begin{bmatrix} \varepsilon_{xx} \\ \varepsilon_{yy} \\ \gamma_{xy} \end{bmatrix}. \quad (8)$$

Computing the laminate strains as a function of stresses, the expressions (8) are:

$$\begin{bmatrix} \varepsilon_{xx} \\ \varepsilon_{yy} \\ \gamma_{xy} \end{bmatrix} = \begin{bmatrix} \underline{c}_{11} & \underline{c}_{12} & \underline{c}_{13} \\ \underline{c}_{12} & \underline{c}_{22} & \underline{c}_{23} \\ \underline{c}_{13} & \underline{c}_{23} & \underline{c}_{33} \end{bmatrix} \cdot \begin{bmatrix} \underline{\sigma}_{xx} \\ \underline{\sigma}_{yy} \\ \underline{\tau}_{xy} \end{bmatrix}, \quad (9)$$

where $\underline{c}_{ij}$ represents the laminate compliance tensor.

It is obvious that the laminate will exhibit different elastic constants if the loading system is applied at a random angle, Φ, to the x-y coordinate system. The compounds of the transformed compliance tensor can be determined in the following way [13]:

$$\underline{c}_{11} = \frac{\cos^4\alpha}{E_{II}} + \frac{\sin^4\alpha}{E_{\perp}} + \frac{1}{4}\cdot\left(\frac{1}{G_{II\perp}} - \frac{2\cdot\upsilon_{\perp II}}{E_{II}}\right)\cdot\sin^2 2\alpha, \quad (10)$$

$$\underline{c}_{22} = \frac{\sin^4\alpha}{E_{II}} + \frac{\cos^4\alpha}{E_{\perp}} + \frac{1}{4}\cdot\left(\frac{1}{G_{II\perp}} - \frac{2\cdot\upsilon_{\perp II}}{E_{II}}\right)\cdot\sin^2 2\alpha, \quad (11)$$

$$\underline{c}_{33} = \frac{\cos^2 2\alpha}{G_{II\perp}} + \left(\frac{1}{E_{II}} + \frac{1}{E_{\perp}} + \frac{2\cdot\upsilon_{\perp II}}{E_{II}}\right)\cdot\sin^2 2\alpha, \quad (12)$$

$$\underline{c}_{12} = \frac{1}{4}\cdot\left(\frac{1}{E_{II}} + \frac{1}{E_{\perp}} - \frac{1}{G_{II\perp}}\right)\cdot\sin^2 2\alpha - \frac{\upsilon_{\perp II}}{E_{II}}\cdot\left(\sin^4\alpha + \cos^4\alpha\right), \quad (13)$$

$$\underline{c}_{13} = \left(\frac{2}{E_{\perp}} + \frac{2\cdot\upsilon_{\perp II}}{E_{II}} - \frac{1}{G_{II\perp}}\right)\cdot\sin^3\alpha\cdot\cos\alpha - \\ -\left(\frac{2}{E_{II}} + \frac{2\cdot\upsilon_{\perp II}}{E_{II}} - \frac{1}{G_{II\perp}}\right)\cdot\cos^3\alpha\cdot\sin\alpha, \quad (14)$$

$$\underline{c}_{23} = \left(\frac{2}{E_{\perp}} + \frac{2\cdot\upsilon_{\perp II}}{E_{II}} - \frac{1}{G_{II\perp}}\right)\cdot\cos^3\alpha\cdot\sin\alpha - \\ -\left(\frac{2}{E_{II}} + \frac{2\cdot\upsilon_{\perp II}}{E_{II}} - \frac{1}{G_{II\perp}}\right)\cdot\sin^3\alpha\cdot\cos\alpha. \quad (15)$$

This tensor can be computed as a function of elastic constants. Thus [14]:

$$E_x = \frac{1}{\underline{c}_{11}}; \quad G_{xy} = \frac{1}{\underline{c}_{33}}; \quad \upsilon_{xy} = -E_x\cdot\underline{c}_{12}. \quad (16)$$

3. Results

All simulations of the elastic properties of fibre-reinforced composite laminates have been carried out using an approach developed by Clyne and Withers from the Department of Materials Science within the Cambridge University, UK [14]. In simulations, following HM-carbon, HS-carbon and Kevlar49 fibres-reinforced laminates have been used: [0/90/0/90], [0/45/-45/90] and [45/-45/45/-45]. For E-glass fibres-reinforced laminates, following plies sequence have been used: [16/-81.8], [30/-30/90] and [55/-55]. General input data are: fibres volume fraction φ = 0.5 in all cases, plies thickness t = 0.125 mm and off-axis loading systems varies between 0 and 90 degrees. For HM carbon fibres, following input data have been used:

- E_M = 3.9 GPa,
- $E_{\|}$ > 300 GPa,
- $E_{\perp}$ < 100 GPa,
- υ_M < 0.5,
- υ_F < 0.4,
- G_M < 25 GPa,
- G_F < 50 GPa.

For HS carbon fibres the input data are:

- $E_{\|}$ < 300 GPa,
- $E_{\perp}$ < 80 GPa.

For Kevlar49 fibres:

- $E_{\|}$ < 200 GPa,
- $E_{\perp}$ < 50 GPa.

For the E-glass fibre-reinforced laminates, following data have been used:

- E_M = 3.9 GPa;
- E_F = 73 GPa;
- υ_M = 0.38;
- υ_F = 0.25;
- G_M < 10 GPa;
- G_F < 25 GPa.

The distributions of the elastic constants E_x, G_{xy} and υ_{xy} for carbon and aramid fibres laminates are presented in Figs. 1-9. The elastic constants E_{xx}, E_{yy}, G_{xy} and υ_{xy} as well as the $\underline{c}_{33}$ distributions for the glass fibres laminates are viewed in Figs. 10 – 14.

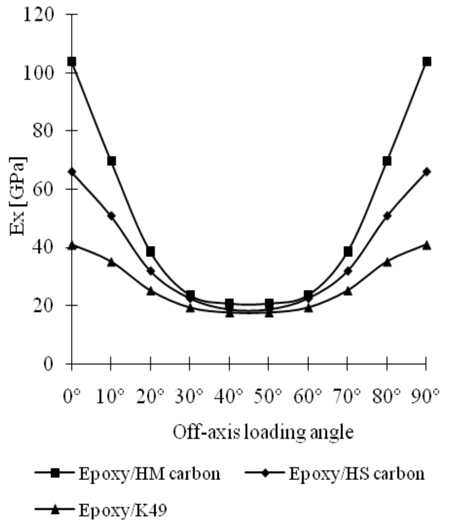

Fig. 1. E_x Young modulus for a [0/90/0/90] epoxy based composite laminate.

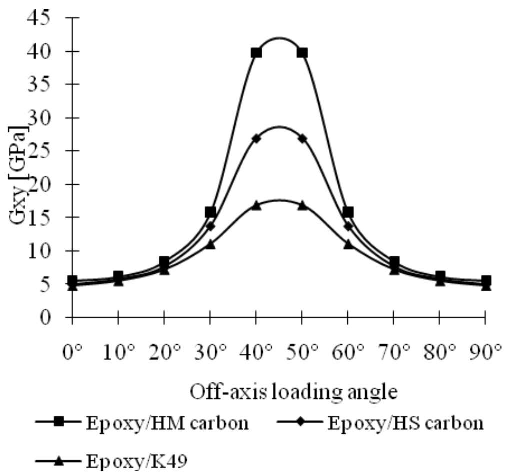

Fig. 2. G_{xy} shear modulus for a [0/90/0/90] epoxy based composite laminate.

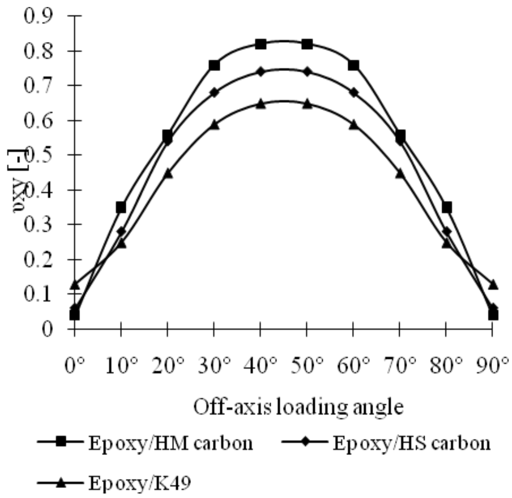

Fig. 3. υ_{xy} Poisson ratio for a [0/90/0/90] epoxy based composite laminate.

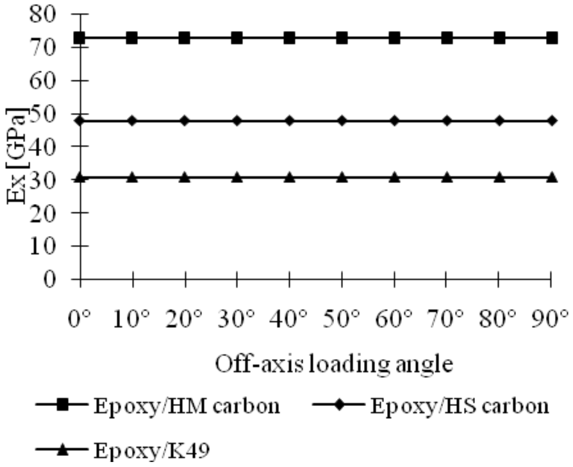

Fig. 4. E_x Young modulus for a [0/45/-45/90] epoxy based composite laminate.

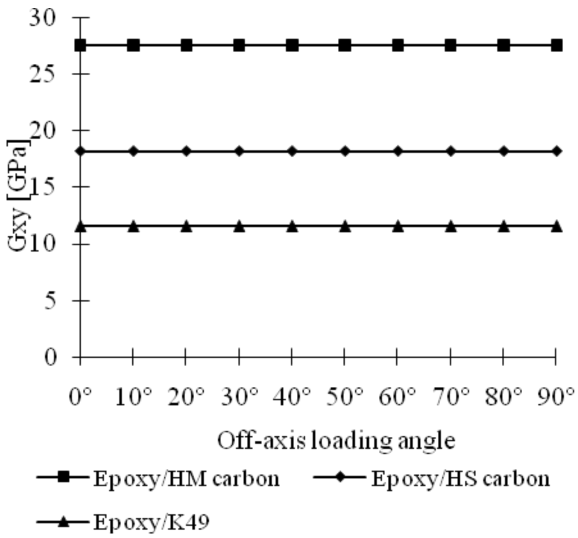

Fig. 5. G_{xy} shear modulus for a [0/45/-45/90] epoxy based composite laminate.

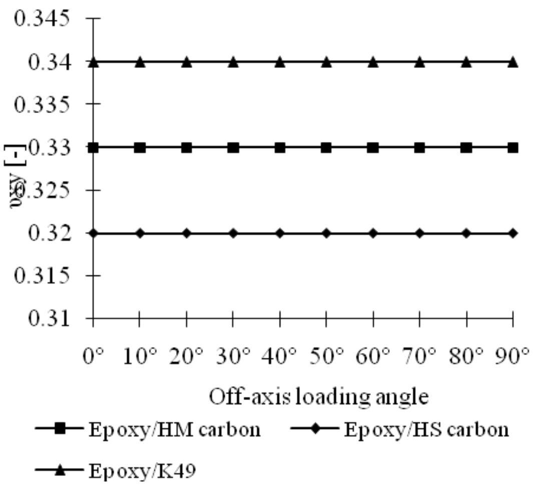

Fig. 6. υ_{xy} Poisson ratio for a [0/45/-45/90] epoxy based composite laminate.

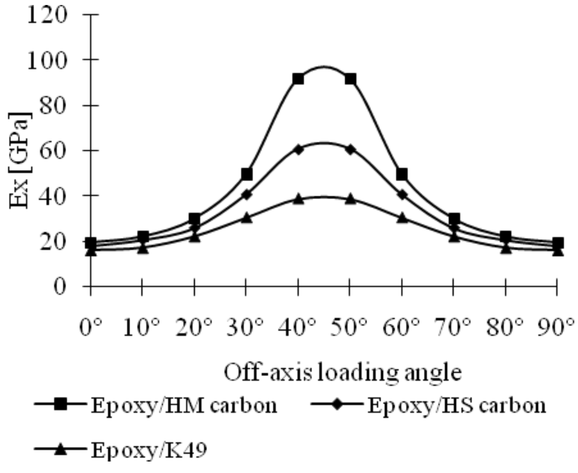

Fig. 7. E_x Young modulus for a [45/-45/45/-45] epoxy based composite laminate.

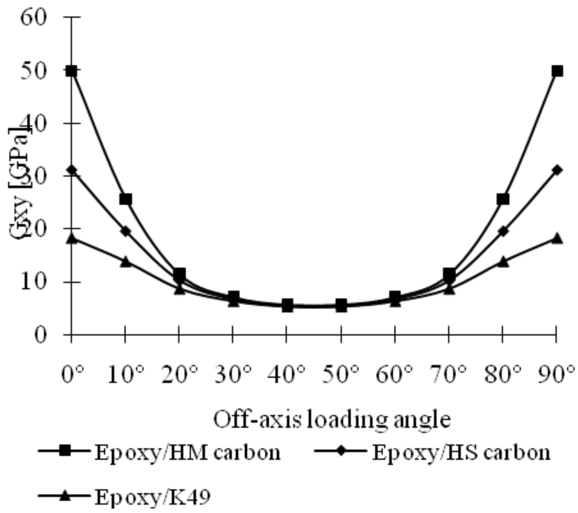

Fig. 8. G_{xy} shear modulus for a [45/-45/45/-45] epoxy based composite laminate.

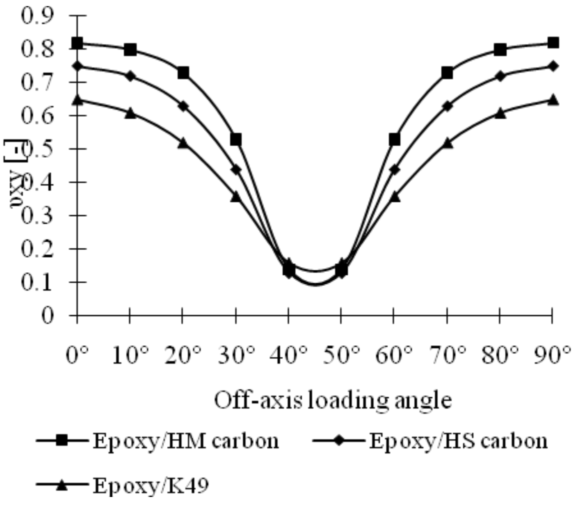

Fig. 9. υ_{xy} Poisson ratio for a [45/-45/45/-45] epoxy based composite laminate.

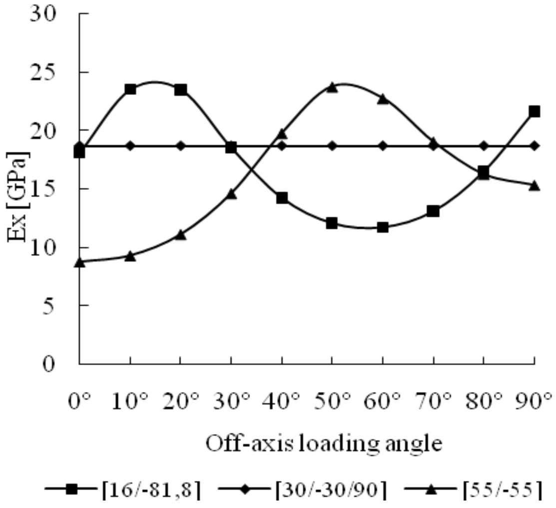

Fig. 10. E_x Young modulus of three epoxy based glass-fibres composite laminates.

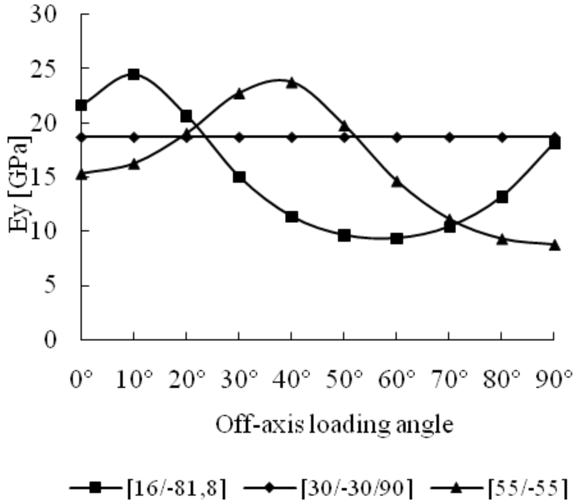

Fig. 11. E_y Young's modulus of three epoxy based glass-fibres composite laminates.

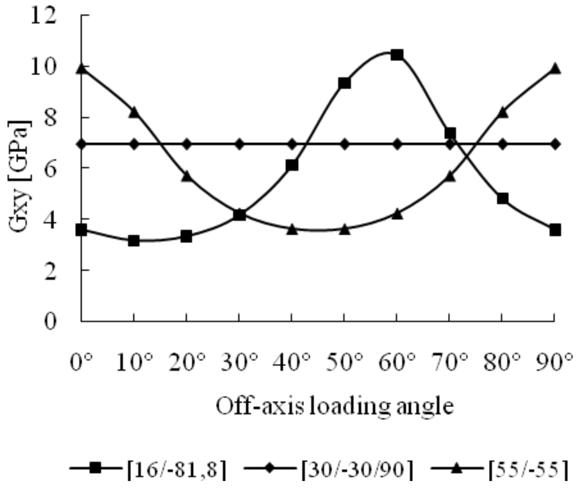

Fig. 12. Shear modulus distribution of three epoxy based glass-fibres composite laminates.

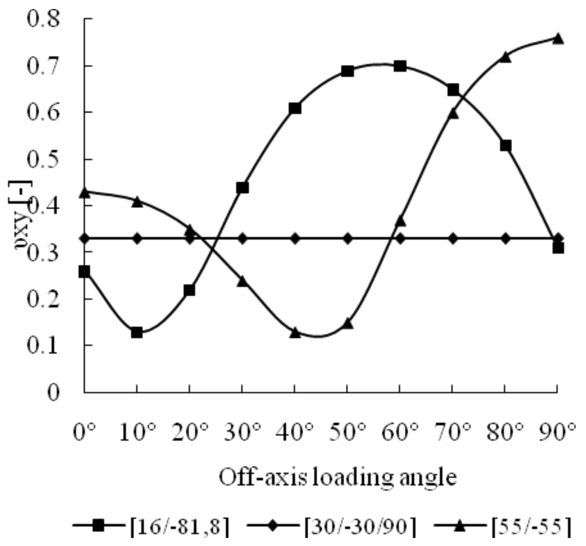

Fig. 13. Poisson ratio distribution of three epoxy based glass-fibres composite laminates.

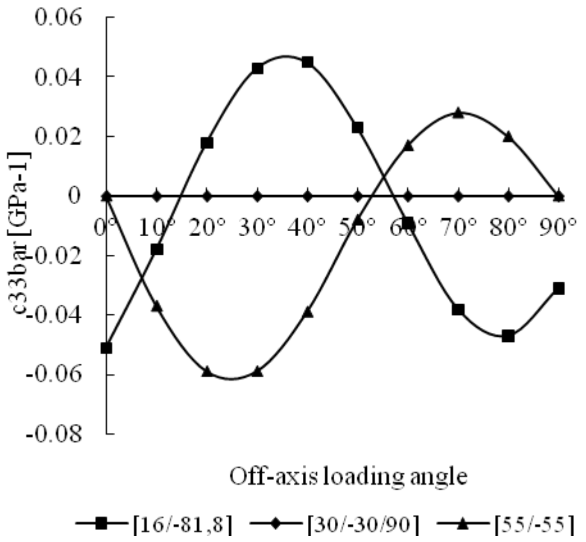

Fig. 14. Distribution of $\underline{c}_{33}$ compound of the transformed compliance tensor.

4. Discussion

Figs. 10 – 13 show an equal stiffness distribution for the laminate with the plies sequence [30/-30/90], which means that this laminate provides balanced angle plies. This kind of structure is more suitable for tubes manufacturing subjected to internal pressure than the laminates [16/-81.9] and [55/-55]. Under off-axis loading, normal stresses produce shear strains and of course, normal strains and shear stresses produce normal strains as well as shear strains.

5. Conclusions

Tensile-shear interactions lead to distortions and local micro-structural damage and failure, so in order to obtain equal stiffness in all off-axis loading systems, a composite laminate have to present balanced angle plies, e.g. [0/45/-45/90]. This tensile-shear interaction is also present in composite laminates (see for instance Fig. 15), but does not occur if the loading system is applied along the main axes of a single lamina or if a laminate is balanced.

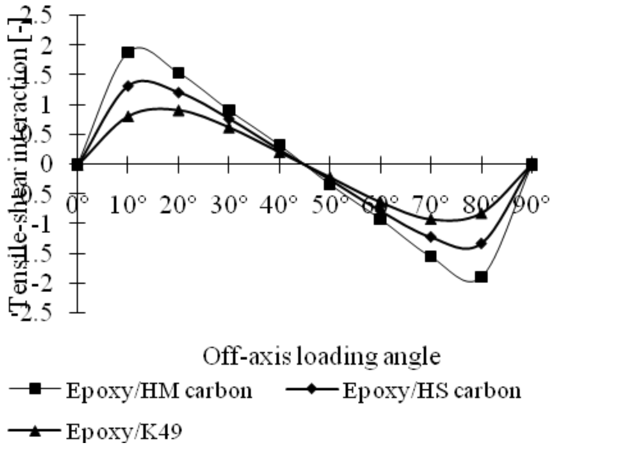

Fig. 15. Distribution of tensile-shear interaction in a [0/90/0/90] composite laminate.

References

[1] D. B. Miracle, R. L. Donaldson, ASM Handbook, Composites, ASM International **21** (2001).
[2] I. M. Daniel, O. Ishai, Engineering of Composite Materials, Oxford University Press, 2nd ed. (2005).
[3] L. C. Bank, Composites for Construction: Structural Design with FRP Materials, Wiley (2006).
[4] D. G. Lee, N. P. Suh, Machine Tools, and Automobiles, Oxford University Press (2005).
[5] A. B. Strong, Society of Manufacturing Engineers, 2nd ed. (2007).
[6] S. Vlase, L. Scutaru, H. Teodorescu, Proc. 6-th Int. DAAAM Baltic Conf. Ind. Eng., Tallin, Estonia, DAAAM International Vienna, 2008, p. 577-582.
[7] J. R. Vinson, R. L. Sierakovski, Springer (2008).
[8] M. F. Ashby, Materials Selection in Mechanical Design, Butterworth-Heinemann, 3rd edition (2005).
[9] A. A. Baker, S. Dutton, D. Kelly, American Institute of Aeronautics & Ast, 2nd ed. (2004).
[10] H. Teodorescu-Draghicescu, S. Vlase, Comp. Mat. Sci., **50**, 4, Feb. (2011).
[11] L. P. Kollar, G. S. Springer, Cambridge University Press (2003).
[12] M. M. Kaminski, Computational Mechanics of Composite Materials: Sensitivity, Randomness and Multiscale Behaviour, Springer, 1st ed. (2004).
[13] M. Knops, Springer (2008).
[14] T. W. Clyne, P. J. Withers, Cambridge University Press (1993).

*Corresponding author: draghicescu.teodorescu@unitbv.ro